Hindawi
International Journal of Photoenergy
Volume 2021, Article ID 6631121, 11 pages
https://doi.org/10.1155/2021/6631121

Research Article

Improvement and Nocturnal Extension of the Efficiency of a Solar Still

Benaissa Mandi,[1] Younes Menni,[1] Rachid Maouedj,[2] Giulio Lorenzini,[3] Mohammad Hossein Ahmadi,[4] and Sampath Emani[5]

[1]*Unit of Research on Materials and Renewable Energies, Department of Physics, Faculty of Sciences, Abou Bekr Belkaid University, P.B. 119-13000 Tlemcen, Algeria*
[2]*Unité de Recherche en Energies Renouvelables en Milieu Saharien (URERMS), Centre de Développement Des Energies Renouvelables (CDER), 01000 Adrar, Algeria*
[3]*Department of Engineering and Architecture, University of Parma, Parco Area delle Scienze, 181/A, Parma 43124, Italy*
[4]*Faculty of Mechanical Engineering, Shahrood University of Technology, Shahrood, Iran*
[5]*Chemical Engineering Department, Universiti Teknologi PETRONAS, 32610 Seri Iskandar, Perak D.R., Malaysia*

Correspondence should be addressed to Mohammad Hossein Ahmadi; mohammadhosein.ahmadi@gmail.com

Received 8 December 2020; Revised 12 February 2021; Accepted 13 May 2021; Published 22 July 2021

Academic Editor: Hafiz Muhammad Ali

Various studies have been made to improve the efficiency of the solar still. These studies had devoted to the combination of solar collectors with solar still. This article proposes the use of all forms of solar thermal or photovoltaic energy. In addition, photovoltaic electric storage systems convert them to thermal energy that increases the temperature of a greenhouse solar still. We investigated the possibility of improving the productivity of a greenhouse still and prolong solar distillation overnight. The proposed system is the incorporation of thermal energy produced by a parabolic-cylindrical concentrator, a greenhouse still, and photovoltaic solar energy by panels. The production at 14 pm reaches 110 L/m^2 thanks to the various thermal sources made up of the hybrid still. It has better productivity than other distillers. The distillation is extended in the evening thanks to a storage system using electric batteries. The production at 18 pm to 18 L/m^2 is reduced at 24 pm to 5 L/m^2 in the dark. The accumulated temperature decreases the negative influence of the physical parameters on the production which exceeds 100 L/m^2 per day. In the evening, the production is reached 16 L/m^2 at 22 pm, which is an advantage compared to other distillers.

1. Introduction

The increase in the volume of pollution disrupts the natural water cycle, causing drought in different areas and lack of water. The problem of water scarcity has worsened over the past centuries, due to careless and heavy consumption of water. In addition to water scarcity, supply of energy is another challenge that should be properly addressed to have better welfare level [1]. Therefore, the use of renewable energy and developing integrated systems are widely discussed and analyzed to answer these problems [2, 3]. Desalination techniques are means that produce water economically in rural and urban areas [4–7]. Research has been done to improve solar desalination (SD) techniques to produce enough water, which can reduce water scarcity. Uses of conventional solar systems, modifications of the heat utilization mechanism are suitable methods to improve the efficiency of the distillation [8]. The most common method is solar distillation [9–11]. Many studies have been done for example; Li et al. [12] used the technique of membrane distillation (MD) through an integrated system by harnessing solar thermal energy. Wang et al. [13] conducted an experimental study for a new design of a seawater distillation system for use in agricultural irrigation. Gopi et al. [14] used radiation energy for sustainable desalination. Muraleedharan et al. [15] designed an active distillation system using solar energy. The performance of this modified system has been compared with the traditional system. Parsa et al. [16]

discussed the influence of different altitudes on the efficiency of solar still. The first height is about 3964 m at the top of Mount Tochal, while the second altitude is estimated at 1171 m for the Tehran city. Miladi et al. [17] studied the technique of recycling hot cooling water, contained to condense the flow, and thus its impact on the efficiency of the vacuum MD station and on its daily production. Hejazi et al. [18] investigated the impact of intermittent operation on the performance of DM. Afzal et al. [19] gave a new system to develop the production of essential oils from plants. Alawee et al. [20–22] augmented the solar distillation yield by using different methods in various geometries. In order to avoid the disadvantages of traditional distillation systems, al-Nimr and Qananba [23] cited another distillation configuration, which relies on a combination of focused optical engineering technique and a nanofluids' spectral-splitting PV/T method. Using the solar distillation (SD) technique, Bhardwaj et al. [24] reported the total water produced with various surfaces of condensation. Kiwan et al. [25] presented a new SD model by developing a conventional power plant for a solar chimney that has the ability to produce both distilled water and electrical energy. Sharshir et al. [26] studied a solar still (SS) integrated in a solar humidification-dehumidification (HDH). The CSS and SS water production with HDH hot water outlet is 37 L/day. Omara et al. [27] analyzed a desalination system using wicks, an evacuated solar water heater, and a solar still. Water productivity has increased by 114% compared to conventional still. Tian and Zhao [28] investigated an examination of solar collectors and thermal energy storage in solar thermal applications. Three different types of concentrated solar collectors have been described and compared: heliostat field collectors, flat parabolic collectors, and trough parabolic collectors. The materials used for high temperature thermal energy storage systems were compared, and a comparison between different categories of thermal storage systems was presented. Molten salts with excellent properties are considered the ideal materials for high temperature thermal storage applications. Ayoub et al. [29] studied a SD system still with productivity. A simple amendment in the form of a slowly rotating drum is introduced allowing the formation of thin layers of water which evaporate quickly and is constantly renewed. The performance of this system was compared to a control without an introduced drum. The system was performed considerably with an average increase in daily productivity of 200%. Abdallah et al. [30] studied solar distillation using a vacuum tube coupled to a photovoltaic system. The system produced 12 L/m^2/day and gave an efficiency of over 60% for more than 5 h in daylight. Sampathkumar et al. [31] reported that many traditional and nontraditional techniques have been developed for distillation. The production is related to the thermal conductivity of coating and condensing materials, and copper has good performance because it has high thermal conductivity. Allouhi [32] studied the progress of thermoelectric solar thermal cogeneration processes and the integration of solar thermoelectric generators in solar thermal collectors. This integration provides thermal and electrical energy, which implies a good control of solar radiation. Dev and Tiwari [33] studied the characteristics of a hybrid solar still (PV-T). A hybrid solar still is a combination of a solar still and a flat plate collector integrated in a glass-to-glass photovoltaic module. It has been observed that the performance of the nonlinear characteristics is better than that of the linear characteristics. Kabeel et al. [34] have studied different types of solar still. The results show that the maximum production is obtained from a solar still with a single slope and pyramidal shape. Qin et al. [35] theoretically studied solar thermal sources of interest for hybrid solar distillation. In another study, Qin [36] provided a measure of the albedo of an urban prototype. They sequentially covered a target area with an opaque white sun mask. They simultaneously measure incident radiation and reflected radiation. Other data in different formulations and subject to distinct conditions have been recently dealt with Sharan et al. [37], Alawee et al. [38, 39], Essa et al. [40], Xiong et al. [41], and Mandi et al. [42].

In this study, we are investigating the possibility of improving productivity and extending nighttime solar distillation using a hybrid solar still and the reduction of the negative impact of weather factors on the production of the solar still. The proposed hybrid still is a coupling system between a greenhouse still, a parabolic cylindro concentrator, and an autonomous photovoltaic generator with a thermal electric converter. These various sources are temperature generators which are used to evaporate the water in the solar still.

2. System Description

Figure 1 illustrates a solar still which was combined with a photovoltaic generator and a parabolic cylindro-parabolic concentrator to have a hybrid system [42]. The operation of this system is based on passive solar energy and the conversion of thermal energy through a cylindro-parabolic concentrator and an autonomous photovoltaic system. The latter supplies converters from electrical energy to thermal energy.

The batteries store electrical energy and keep the system running, at times when the sun's rays are weak. The productivity and the operating time determine the size and the cost of the system. The hybrid system can operate during the additional hours of sunset thanks to the autonomy of the photovoltaic generator.

3. Mathematical Model

3.1. Assumptions. For the calculation of the energy balance, one poses the following:

(i) The fluid is incompressible

(ii) The parabola is symmetrical

(iii) The ambient temperature is uniform

(iv) The glass is opaque to infrared radiation

(v) The flow is one-dimensional

(vi) Temporal variations in the thickness of the absorber and the glass are negligible

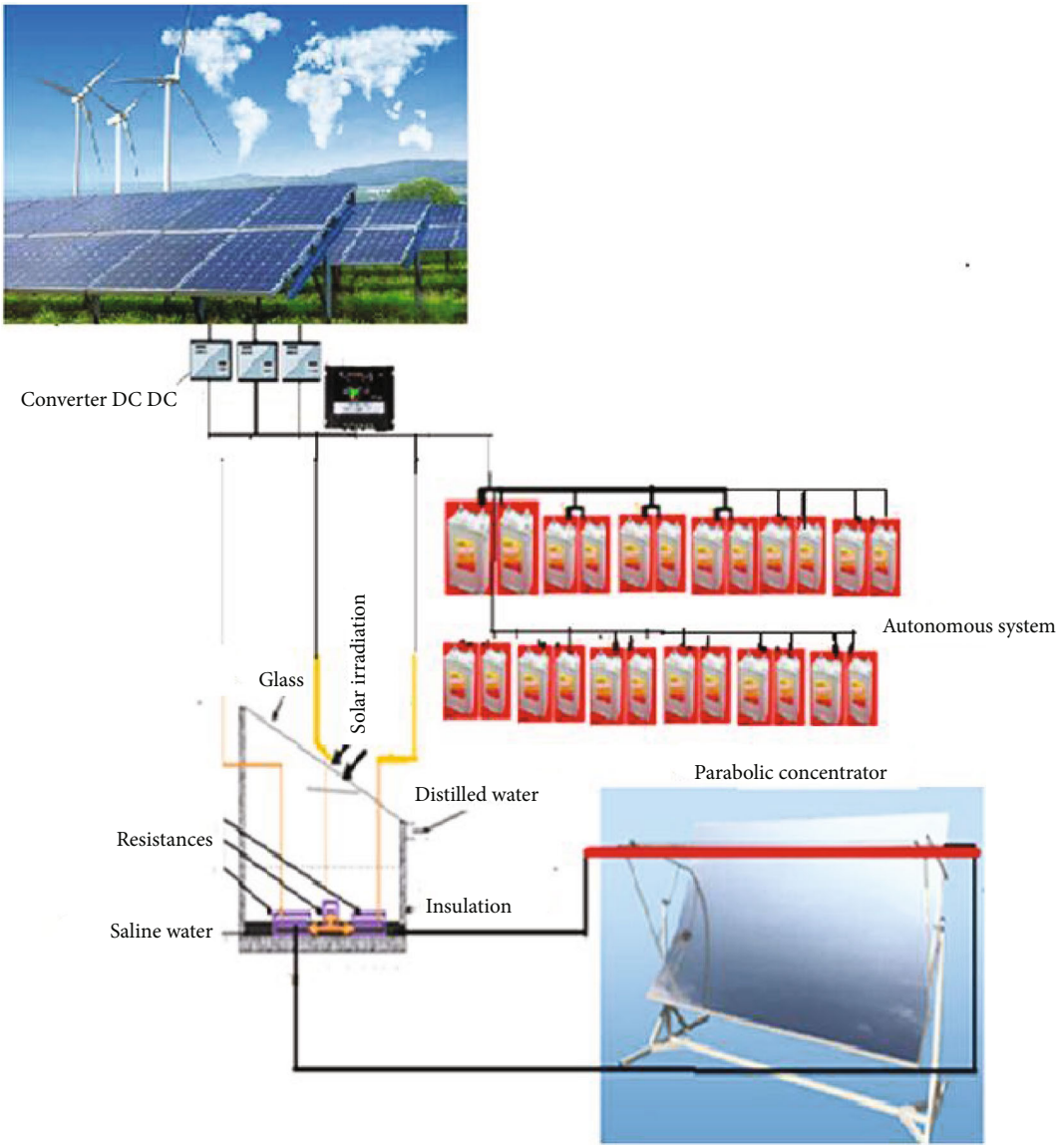

Figure 1: Thermal balance of the absorber tube of the CCP concentrator [42].

(vii) The exchange by conduction in the absorber and the glass is negligible

(viii) The effect of the shadow of the absorber tube on the mirror is negligible

(ix) The solar flux of the absorber is uniform

3.2. Cylindro-Parabolic Concentrator

3.2.1. Energy Balance for the Fluid. The energy balance of the fluid moving in the absorber is [43]

$$\frac{d}{dt}\left(\Delta Q_f(z,t)\right) = q_{\text{inl}}(z,t) - q_{\text{out}}(z+\Delta z,t)\cdot\Delta z. \quad (1)$$

The amount of heat recovered by the fluid $\Delta Q_F(z,t)$ in the interval Δz is

$$\begin{aligned}(\Delta Q_F(z,t)) &= \rho_F - c_F A_{\text{internal}}\cdot\Delta z T_F(z,t),\\ A_{A,\text{internal}} &= \pi\cdot D_{A,i}.\end{aligned} \quad (2)$$

The amount of heat entering and leaving the element of length Δz is

$$q_{\text{entered}}(z,t) = \rho_F C_F V' T_F(z,t),$$

$$q_{\text{entered}}(z+\Delta z,t) = \rho_F C_F V' T_F(z+\Delta z,t),$$

$$\rho_F c_F A_{A,\text{internal}}\cdot\Delta z\frac{dT_F(z,t)}{dt} = \rho_F c_F V'\cdot T_F(z,t) - \rho_F c_F V'\cdot T_F(z+\Delta z,t) + q_{\text{exit}}(z,t). \quad (3)$$

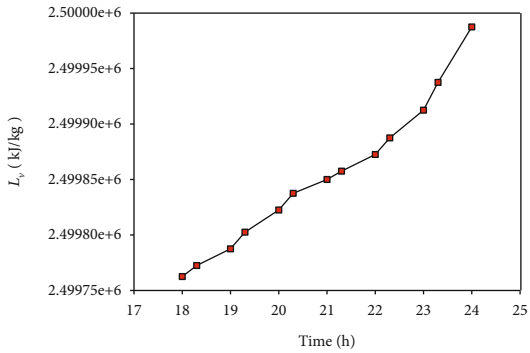

Figure 2: Temporal variation of latent heat of water.

The partial derivative with respect to the abscissa z is

$$\frac{dT_F(z,t)}{\Delta z} = \frac{dT_F(z+\Delta z,t) - T_F(z,t)}{\Delta z}. \quad (4)$$

In divisions by Δz and after substitution, we get

$$\rho_F C_F A_{A,\text{internal}} \frac{dT_F(z,t)}{dt} = -\rho_F c_F V' \cdot \frac{dT_F(z,t)}{dt} + q_{\text{useful}}(z,t). \quad (5)$$

The initial conditions and the boundary conditions are

$$\begin{aligned} T_F(0,t) &= T_{F,\text{entered}}(t) = T_{\text{amb}}(t), \\ T_F(z,0) &= T_{F,\text{initial}}(z) = T_{\text{amb}}(0). \end{aligned} \quad (6)$$

3.2.2. Between the Absorber and the Glass Envelope.

$$\begin{aligned} \frac{dz(\Delta Q_A(z,t))}{dt} &= (q_{\text{absorbed}}(t) - q_{\text{inside}}(z,t) - q_{\text{useful}}(z,t))\Delta z, \\ \Delta Q_{\text{abs}}(z,t) &= A_{\text{abs}} \cdot \rho_{\text{abs}} \cdot C_{\text{abs}} \cdot \Delta z \cdot T_{\text{abs}}(z,t). \end{aligned} \quad (7)$$

The power absorbed per unit of opening area is written as follows:

$$q_{\text{absorbed}} = I \cdot \rho \cdot \tau \cdot C \cdot \gamma. \quad (8)$$

After substitution, we get the following expression:

$$\rho_{\text{abs}} \cdot C_{\text{abs}} \cdot A_{\text{abs}} \frac{dT_{\text{abs}}}{dt} = q_{\text{absorbed}}(t) - q_{\text{inside}}(z,t) - q_{\text{useful}}(z,t). \quad (9)$$

The initial conditions are

$$T_A(z,0) = T_{A,\text{initial}}(z) = T_{\text{amb}}(0). \quad (10)$$

3.2.3. Between the Glass Envelope and the Environment.

$$\rho_v C_v A_v \frac{dT_v(z,t)}{dt} = q_{\text{internal}}(z,t) - q_{\text{external}}(z,t). \quad (11)$$

The amount of external heat between the glazing and the surrounding environment is shown.

The initial condition is as follows:

$$T_g(z,0) = T_{g,\text{initial}}(z) = T_{\text{amb}}(0). \quad (12)$$

3.3. Green House Distiller. Figure 1 (part B) illustrates the different heat exchanges that occur in a solar still. The equations, which express the heat balance at the level of each part of the still [44], are written as follows:

(i) In the cover:

(a) Outside:

$$\frac{M_g}{2} \cdot \frac{cp_g}{A_g} \cdot \frac{dT_{ge}}{dt} + q^c_{g-a} + q^r_{g-a} = \frac{\lambda_g}{e_g} \cdot \left(T_{gi} - T_{ge}\right) \quad (13)$$

(b) Inner face:

$$\frac{M_g}{2} \cdot \frac{cp_g}{A_g} \cdot \frac{dT_{gi}}{dt} + \frac{\lambda_g}{e_g} \cdot \left(T_{gi} - T_{ge}\right) = q^c_{w-g} + q^r_{w-g} + q^{ev}_{w-g} + P_g \quad (14)$$

(ii) In the brine:

$$M_w \cdot \frac{cp_w}{A_w} \cdot \frac{dT_w}{dt} + q^c_{w-g} + q^r_{w-g} + q^{ev}_{w-g} = p_w + q^c_{b-w} \quad (15)$$

(a) In the absorbent tray:

$$M_b \cdot \frac{cp_b}{A_b} \cdot \frac{dT_b}{dt} + q^c_{b-w} + q^{cd}_{b-isi} = pb \quad (16)$$

(iii) In the insulation:

To reduce heat loss through the base, we use thermal insulation. The inner side of the still receives the heat lost from the absorber and the outer side releases heat to the outside by radiation and convection, hence the equation:

(a) Inner face:

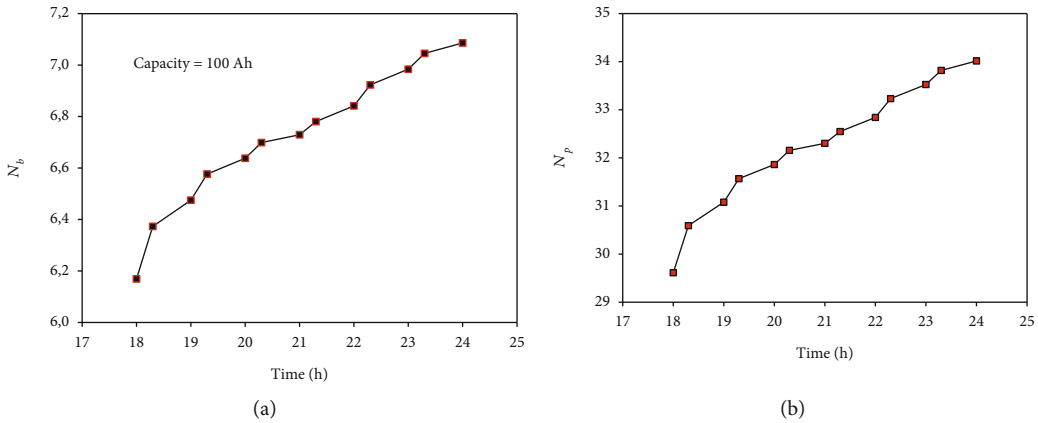

(a) (b)

Figure 3: Variation of number of (a) batteries and (b) panels as a function of time of distillation.

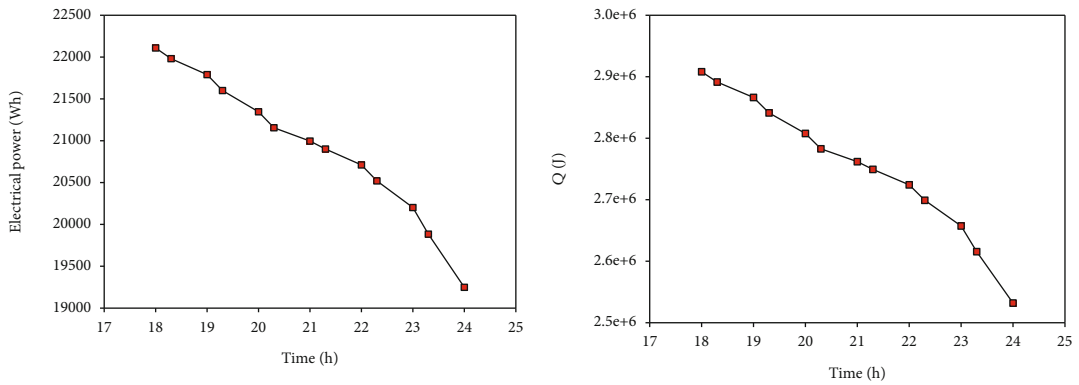

(a) (b)

Figure 4: Temporal variation of (a) electric power and (b) thermal power.

$$\frac{M_{\text{is}}}{2} \cdot \frac{cp_{\text{is}}}{A_{\text{is}}} \cdot \frac{dT_{isi}}{dt} + \frac{\lambda_{\text{is}}}{e_{\text{is}}} \cdot (T_{isi} - T_{ise}) = q^{cd}_{b-isi} \tag{17}$$

(b) Outside face:

$$\frac{M_{\text{is}}}{2} \cdot \frac{cp_{\text{is}}}{A_{\text{is}}} \cdot \frac{dT_{ise}}{dt} + q^{c}_{\text{is}-a} + q^{r}_{\text{is}-a} = \frac{\lambda_{\text{is}}}{e_{\text{is}}} \cdot (T_{isi} - T_{ise}) \tag{18}$$

3.4. Hybrid Distiller.

$$M_w \frac{cp_w}{A_w} \frac{dT_w}{dt} + q^{c}_{w-g} + q^{r}_{w-g} + q^{er}_{w-g} = p_w + mcp(T_{cc} - T_{w0}) + mcp(T_{el} - T_{w0}) + q^{c}_{b-w}. \tag{19}$$

3.5. Estimated Consumption. The power of all the devices that will be part of the installation must be determined individually, as well as the average duration of use of each of them [45]:

The alternating and direct current devices will be

$$E_{AC} = \sum P_{(AC)i} \cdot t_{di},$$
$$E_{DC} = \sum P_{(DC)i} \cdot t_{di}, \tag{20}$$
$$E_T = \frac{E_{DC}}{\eta_{\text{BAT}}} + \frac{E_{AC}}{\eta_{\text{BAT}} \cdot \eta_{\text{INV}}}.$$

3.6. Dimensioning of the Photovoltaic Generator. The total number of photovoltaic modules to be installed can be calculated from the following expression [46]:

$$N_T = \frac{E_T}{P_p G_{m\beta} P_G}. \tag{21}$$

The number of modules to be connected in series is calculated as follows:

$$N_S = \frac{V_{\text{Bat}}}{V_m}. \tag{22}$$

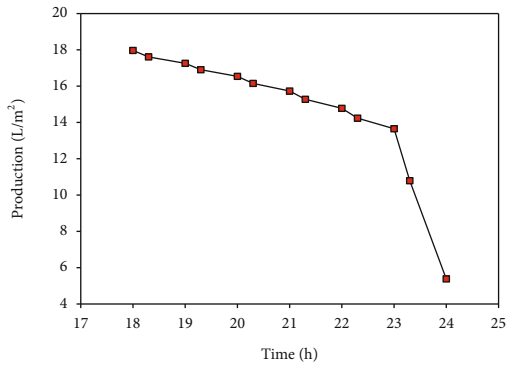

Figure 5: Temporal variation of the production of the autonomous hybrid distiller.

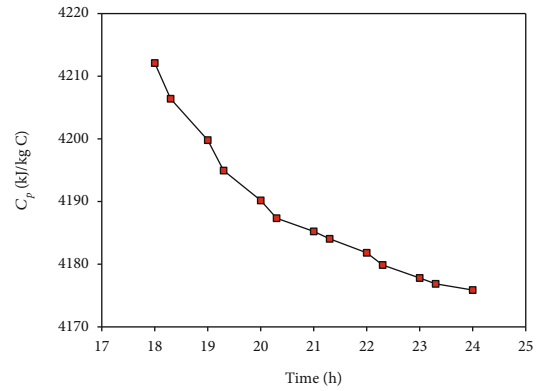

Figure 6: Temporal variation of the specific heat of water.

The number of modules connected in parallel is

$$N_S = \frac{V_{\text{Bat}}}{V_m}. \tag{23}$$

3.7. Autonomy. To define the size of the accumulator, the following parameters must be taken into account:

3.7.1. Maximum Discharge Depth. This is the maximum level of discharge that is allowed to the battery before disconnecting the regulator.

3.7.2. Autonomy Days. This is the number of consecutive days in the absence of sunlight. The accumulation system is able to respond to consumption, without exceeding the maximum depth of discharge of the battery [47].

$$\begin{aligned} C_n(Wh) &= \frac{E_T N}{P_d}, \\ C_n(Ah) &= \frac{C_n(Wh)}{V_{\text{Bat}}}. \end{aligned} \tag{24}$$

3.8. Sizing of the Regulator. The main purpose of the regulator is to obtain the maximum current that will flow through the installation. We need to calculate the current produced by the generator, the current that consumes the load. The maximum of these two currents will be at which the regulator must withstand in operation:

$$\begin{aligned} I_G &= I_R \cdot N_R, \\ I_R &= \frac{P_p \eta_m}{V_m}. \end{aligned} \tag{25}$$

The intensity consumed by the load is determined taking into account all the consumptions at the same time:

$$I_C = \frac{P_{DC}}{V_{\text{batm}}} + \frac{P_{AC}}{220}. \tag{26}$$

The regulator will have to withstand the maximum of the two currents which will be used for its election.

$$I_R = \max\left(I_G, I_C\right). \tag{27}$$

3.9. Dimensioning of the Converter. The operating characteristics that define an inverter or converter are DC-AC:

(i) Rated power

(ii) Input voltage

(iii) Rated output voltage

(iv) Operating frequency

(v) Performance

The power demanded by the AC load will be taken into account, so an inverter with a rated power slightly higher than the maximum will be chosen.

3.9.1. The Expression of the Power of the Inverter.

$$P_{Rinv} \approx P_{AC}. \tag{28}$$

3.10. Dimensioning of the Wiring. In the load power cables, there will be losses due to voltage drops. These ohmic losses must meet the restrictive of the following two conditions:

(1) The low voltage electrotechnical standards must be checked

(2) The energy loss must be less than a predefined amount

Its value can be calculated with the following expressions:

$$\begin{aligned} P_{PC} &= I^2 \cdot R_c, \\ R_c &= \frac{\rho \cdot L}{S}. \end{aligned} \tag{29}$$

3.11. Conversion of Electrical Energy to Thermal Energy. The system consists of a photovoltaic network which produces electrical energy feed heating resistors, which convert

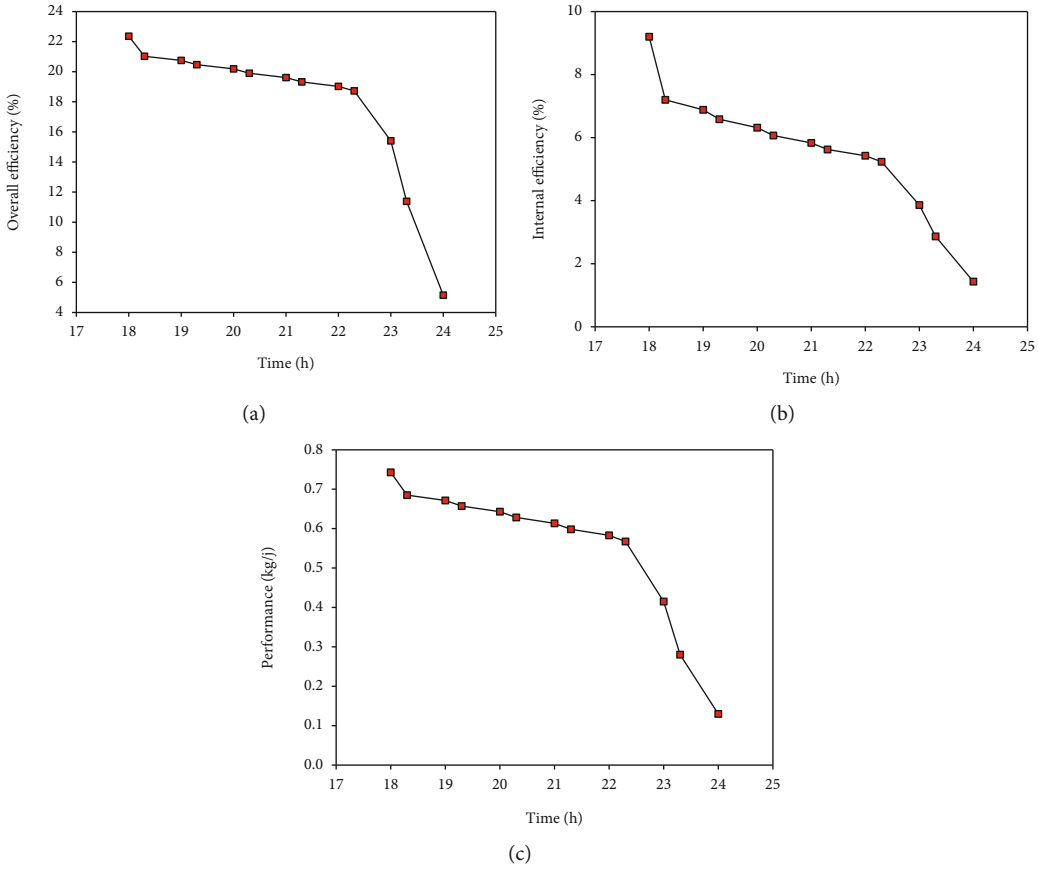

Figure 7: Temporal variation of (a) global efficiency, (b) internal efficiency, and (c) performance.

electrical energy into thermal energy.

$$\begin{aligned} Q &= m \cdot Cp \cdot \Delta T, \\ P &= V \cdot R = R \cdot I^2, \\ Q &= P \cdot \Delta t, \\ \Delta T &= \frac{P \cdot \Delta t}{m \cdot Cp}. \end{aligned} \tag{30}$$

4. Results and Discussion

Figure 2 shows the temporal variation of latent heat during the evening. At 6 pm, the latent heat is at the minimum because the temperature is high, but at 24 pm, the latent heat is at the maximum because the temperature is at the minimum. It is concluded that the temperature influences the latent heat inversely.

Figures 3(a) and 3(b) show the temporal variation of the following parameters: the number of batteries and the number of panels, respectively. From 18 pm to 24 pm, the storage system produces the temperature overnight. It is noted that the number of photovoltaic elements increases, due to the temperature requested during the night.

Figures 4(a) and 4(b) show the temporal variation of thermal power and electric power, respectively. At 18 pm, thermal and electrical powers are high due to thermal storage. From 18 pm to 24 pm, they are weak because of the solar radiation, which is zero.

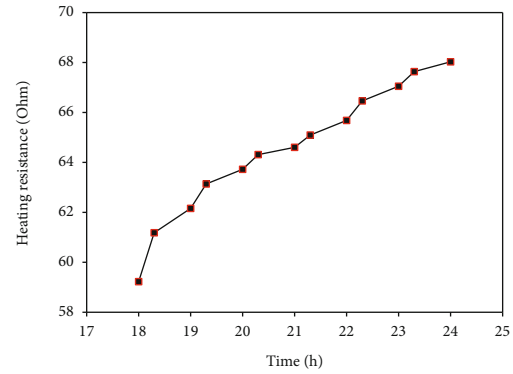

Figure 8: Temporal variation of the electrical resistance.

Figure 5 shows the variation in production over time. It is maximum at 18 pm due to the high thermal power generated by several energy sources in the system. From 18 pm to 24 pm, production decreases up to 24 h because the electrical storage is exhausted.

Figure 6 shows the temporal variation of the specific heat of water which hangs from maximum values at 18 pm, then

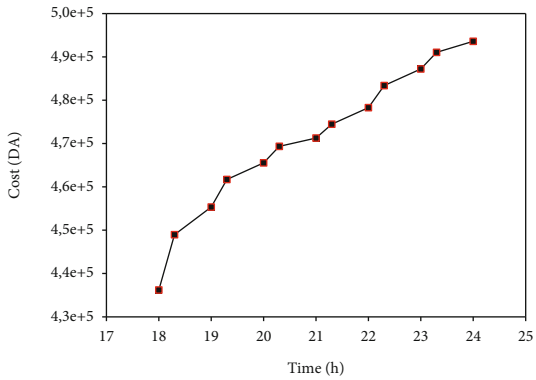

Figure 9: Variation of installation cost as a function of time.

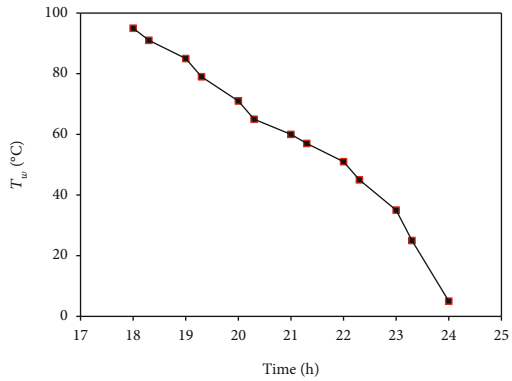

Figure 10: Variation of water temperature at sunset.

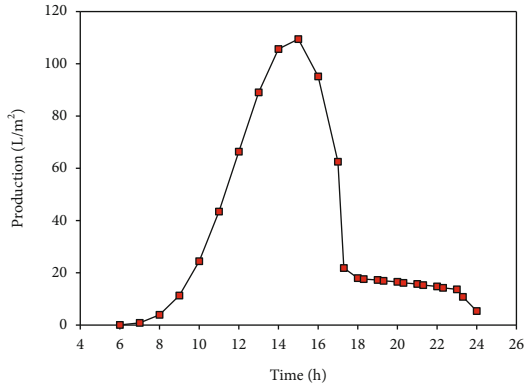

Figure 11: Temporal variation of the production of the hybrid distiller coupled with CCP and the system of autonomy.

decreases to minimum values at 24 pm, due to the temperature, which is low at 24 pm.

Figures 7(a)–7(c) show the temporal variation of the overall efficiency, internal efficiency, and performance, respectively, which hang from maximum values at 18 pm. These settings decrease slightly from 18 pm to 10 pm due to the stored temperature. From 10 pm to 24 pm, the above items decrease rapidly, as the temperature decreases to minimum values.

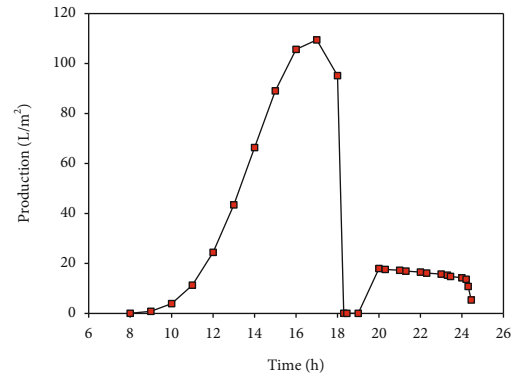

Figure 12: Effect of the delay of operation of the autonomy on the temporal variation of the production of the distiller coupled with a CCP and the autonomy.

Figure 8 shows the variation in electrical resistance which converts electrical energy stored by batteries to thermal energy overnight. A 68-ohm resistor maintains the distillation temperature for up to 24 hours. From 6 pm to midnight, we observe the evolution of the cost of distillation during the night.

Figure 9 shows that the time and amount of distillation increase the number of batteries and solar panels. In addition, the cost increases due to the number of the two previous parameters.

Figure 10 shows the temporal variation of the water temperature. At 18 pm, the temperature is high due to multiple energy sources and heat build-up. From 18 pm to 24 pm, the temperature decreases slowly thanks to the energy stored up to 24 pm.

Figure 11 shows the variation in production over time. From 12 pm to 14 pm, production reaches 100 L/m^2, because the solar radiation is powerful. At 18 pm, the production is almost 20 L/m^2 due to the absence of solar radiation. From 18 pm to 24 pm, the production is less than 20 L/m^2 during the night, due to the autonomy of the system.

Figure 12 shows the temporal variation of the production with a stop of operation of the autonomy which illustrated in the diagram from 18 h to 19 h. Then, the autonomy system begins to operate from 19 pm to midnight, which is why production grows at an average value of 16 L/m^2. At 23 pm, production slowly decreases to 0 L/m^2 at 24 pm, as the electrical energy storage is depleted.

Figure 13 shows the variation over time in the production of the following distillers: greenhouse still, hybrid still, hybrid still coupled to the CCP, and hybrid still coupled to the CCP and the autonomy system. The latter is the most efficient than the others and offers the advantage of night distillation from 18 pm to midnight.

5. Validations

Two experimental have been made on the coupling which shows that this method is effective in increasing the efficiency of solar stills. Elbar and Hassan [48] experimented with the coupling of a photovoltaic module and the integration of

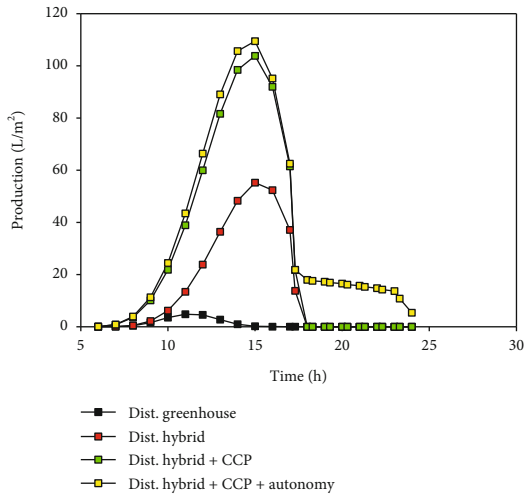

Figure 13: Temporal variation of the production of distillers.

phase change materials with the conventional solar tank (CSS). The results indicate that the combination of PV with CSS increases its production by 9%. Using the phase change pole with the PV coupled still increases their daily efficiency to 11.7%. Fathy et al. [49] experimentally studied the performance of coupling a parabolic collector with a double slope solar still. The results show that the solar still with the parabolic collector has a higher output than the conventional solar still. Freshwater production from the solar still with the parabolic collector followed about 142.3% at a saltwater depth of 20 mm in summer.

6. Conclusion

Combining several solar energy sources in one system, it improves and prolongs solar distillation at night. The coupling of concentrators or solar collectors and photovoltaic energy produces powerful thermal energy. It increases the thermal power of the passive still and improves its efficiency. The production reaches the maximum of 100 L/m^2 from noon to 14 pm, because the solar radiation is strong. From 16 pm to 18 pm, the production decreases to 20 L/m^2, due to the weak solar rays. From 18 pm to 24 pm, the production of the still takes average values thanks to the autonomy of the system. From 18 pm to 19 pm, a time difference is clearly visible in the production diagram due to an autonomy malfunction. From 19 pm to 24 pm, the autonomy system resumes operation and production increases to average values. Finally, the hybrid still, coupled with the CCP and an autonomous system, is more efficient than the other distillers proposed by various researches. In addition, it offers an advantage of distillation which lasts from 18 pm to 24 pm. The results show that the coupling of different thermal sources has several advantages for solar distillation. For example, it improves productivity, decreases the effect of meteorological factors on production, and prolongs the production time of the greenhouse still. From the study, it was noticed that thermal electrical conversion is a necessary factor that can improve still productivity to values of great interest for hybrid solar distillation.

Nomenclature

Ai: Surface of a body of index i (m^2)
C_n: Nominal battery capacity (Wh or Ah)
Cp_i: The specific heat of material of index i (J·kg^{-1}°C^{-1})
E_{AC}: Energy consumed in alternating current (Wh)
E_{DC}: Energy consumed in direct current (Wh)
e_g: Glass thickness (m)
e_{is}: Insulation thickness (mm)
E_{prod}: Produced electric energy (Wh)
E_T: Actual energy required by the system (consumption) (Wh)
g: Acceleration (m·s^{-2})
G_{mb}: Global radiation on a surface inclined at an angle b (kWh·m^{-2})
Gr: Grashof number
h_m: Nominal voltage of the modules (V)
I: Current intensity (A)
IG: Solar irradiation (W·m^{-2})
I_G: Generator current (A)
I_R: Parallel branch current of generator (A)
Kv: Coefficient of extinction of the glass (m^{-1})
L: Conductor length (m)
L_v: Latent heat of vaporization (J·kg^{-1})
m: Mass (kg)
m_A: Mass flow rate (kg·s^{-1})
M_c: Mass of the condensate (kg·s^{-1})
m_d: Mass flow rate of distillate (kg·s^{-1})
M_w: Molecular weight (g·mol^{-1})
N: Number of hours of exposure drum module (h)
N_p: Being the number of modules to be connected in parallel branches
N_R: Number of parallel branches of the generator
Ns: Number of modules in series per branch
$P^w{}_v$: Spray pressure to T_w
P_b: Solar power absorbed by the absorber (W·m^{-2})
P_c: Peak power (W)
P_d: Maximum depth of battery discharge
P_g: Solar power absorbed by the glass (W·m^{-2})
P_G: Overall loss factor (generally varies between 0.65 and 0.9)
P_i: Solar power absorbed by the body of index i (W·m^{-2})
P_p: Peak power of the module (W·m^{-2})
P_{PC}: Current flowing through the conductors (A)
Pr: Number of Prandtl
P_w: Energy absorbed by water (W·m^{-2})
$q_{absorbed}$: The amount of solar energy absorbed from thermodynamics we have (W)
$q^c{}_{b-isi}$: Heat flux between the bin and the water (W)
$q^{cd}{}_{b-isi}$: Heat flux lost by conduction from the tank (W)
$q^c{}_{g-a}$: Heat flow lost by convection through the glass to the outside (W)
$q^c{}_{is-a}$: Heat flow lost by conduction (W)
$q^c{}_{w-g}$: Heat flux by convection between the film of water and the glass (W)

Q_{E24h}: Quantity of energy entered after 24 hours (W)
Q_{ev}: Amount of heat used for evaporation per unit of time (useful gain) (W)
$q^{ev}{}_{w-g}$: Heat flux by condensation between the water film and the glass (W)
$q_{external}$: Amount of heat lost to the outside (W)
q_{inside}: The amount of energy that indicates the heat transfer between the absorber tube and the glass envelope (W)
$q_{internal}$: Quantity of internal heat in the annular space (W)
Q_{P24h}: Quantity of water produced after 24 hours (W)
$q^{r}{}_{g-a}$: Heat flux lost by the glass by radiation to the outside (W)
$q^{r}{}_{is-a}$: Heat flux by radiation between the insulation and to the outsides (W)
$q^{r}{}_{w-g}$: Heat flux by radiation (W)
q_{useful}: Heat flow exchanged by convection between the absorber and the fluid (W)
$q^{w}{}_{v}$: Spray pressure to T_w
R_C: Ohmic resistance of conductors (Ohm)
S: Conductor cross section (mm^2)
t_{di}: Daily use time (h)
T_i: Body temperature of index i (°C)
V_{Bat}: Nominal battery voltage (V)
V_m: Nominal voltage of the modules (V)
z: Tube length (mm)
α_a: Absorption coefficient of transmission
α_b: Coefficient of absorption by the basin
Δz: Element length (mm)
ε_g: Emission of the glass
ε_w: Water emissivity
λ_i: Thermal conductivity of material of index i ($W{\cdot}m^{-1}{}^{\circ}C^{-1}$)
ρ: Density $(kg{\cdot}m^{-})^3$
ρ_r: Transmission coefficient due to reflection
σ: Stefan-Boltzmann constant ($Wm^{-2}{\cdot}K^{-4}$)
τ_w: Coefficient of transmission of brine.

Data Availability

Only we can provide the results reported in the article to other researchers.

Conflicts of Interest

The authors declare that they have no conflicts of interest.

References

[1] B. Ghorbani, Z. Javadi, S. Zendehboudi, and M. Amidpour, "Energy, exergy, and economic analyses of a new integrated system for generation of power and liquid fuels using liquefied natural gas regasification and solar collectors," *Energy Conversion and Management*, vol. 219, article 112915, 2020.

[2] M. Nouri, M. Miansari, and B. Ghorbani, "Exergy and economic analyses of a novel hybrid structure for simultaneous production of liquid hydrogen and carbon dioxide using photovoltaic and electrolyzer systems," *Journal of Cleaner Production*, vol. 259, article 120862, 2020.

[3] A. Ebrahimi, B. Ghorbani, and M. Ziabasharhagh, "Introducing a novel integrated cogeneration system of power and cooling using stored liquefied natural gas as a cryogenic energy storage system," *Energy*, vol. 206, article 117982, 2020.

[4] V. S. Gupta, D. B. Singh, R. K. Mishra, S. K. Sharma, and G. N. Tiwari, "Development of characteristic equations for PVT-CPC active solar distillation system," *Desalination*, vol. 445, pp. 266–279, 2018.

[5] H. Manchanda and M. Kumar, "Performance analysis of single basin solar distillation cum drying unit with parabolic reflector," *Desalination*, vol. 416, pp. 1–9, 2017.

[6] B. Ghorbani, M. Miansari, S. Zendehboudi, and M.-H. Hamedi, "Exergetic and economic evaluation of carbon dioxide liquefaction process in a hybridized system of water desalination, power generation, and liquefied natural gas regasification," *Energy Conversion and Management*, vol. 205, article 112374, 2020.

[7] A. Ebrahimi, B. Ghorbani, M. Ziabasharhagh, and M. J. Rahimi, "Biomass gasification process integration with Stirling engine, solid oxide fuel cell, and multi-effect distillation," *Journal of Thermal Analysis and Calorimetry*, 2020.

[8] B. Ghorbani, R. Shirmohammadi, M. Amidpour, F. Inzoli, and M. Rocco, "Design and thermoeconomic analysis of a multi-effect desalination unit equipped with a cryogenic refrigeration system," *Energy Conversion and Management*, vol. 202, article 112208, 2019.

[9] F. A. Essa, W. H. Alawee, S. A. Mohammed, A. S. Abdullah, and Z. M. Omara, "Enhancement of pyramid solar distiller performance using reflectors, cooling cycle, and dangled cords of wicks," *Desalination*, vol. 50, article 115019, 2021.

[10] H. A. Dhahad, W. H. Alawee, and T. A. Mohammad, "Review on the important methods used to enhance the productivity of the solar still," *International Journal of Scientific & Engineering Research*, vol. 8, no. 7, pp. 12–18, 2017.

[11] W. H. Alawee, S. A. Mohammed, H. A. Dhahad, A. S. Abdullah, Z. M. Omara, and F. A. Essa, "Improving the performance of pyramid solar still using rotating four cylinders and three electric heaters," *Process Safety and Environmental Protection*, vol. 148, pp. 950–958, 2021.

[12] Q. Li, L.-J. Beier, J. Tan et al., "An integrated, solar-driven membrane distillation system for water purification and energy generation," *Applied Energy*, vol. 237, pp. 534–548, 2019.

[13] Q. Wang, S. Liang, Z. Zhu, G. Wu, Y. Su, and H. Zheng, "Performance of seawater-filling type planting system based on solar distillation process: numerical and experimental investigation," *Applied Energy*, vol. 250, pp. 1225–1234, 2019.

[14] G. Gopi, G. Arthanareeswaran, and A. F. Ismail, "Perspective of renewable desalination by using membrane distillation," *Chemical Engineering Research and Design*, vol. 144, pp. 520–537, 2019.

[15] M. Muraleedharan, H. Singh, M. Udayakumar, and S. Suresh, "Modified active solar distillation system employing directly absorbing Therminol 55-Al_2O_3 nano heat transfer fluid and Fresnel lens concentrator," *Desalination*, vol. 457, pp. 32–38, 2019.

[16] S. M. Parsa, D. Javadi Y, A. Rahbar et al., "Experimental assessment on passive solar distillation system on Mount Tochal at the height of 3964 m: study at high altitude," *Desalination*, vol. 466, pp. 77–88, 2019.

[17] R. Miladi, N. Frikha, A. Kheiri, and S. Gabsi, "Energetic performance analysis of seawater desalination with a solar

membrane distillation," *Energy Conversion and Management*, vol. 185, pp. 143–154, 2019.

[18] M.-A. A. Hejazi, O. A. Bamaga, M. H. Al-Beirutty, L. Gzara, and H. Abulkhair, "Effect of intermittent operation on performance of a solar-powered membrane distillation system," *Separation and Purification Technology*, vol. 220, pp. 300–308, 2019.

[19] A. Afzal, A. Munir, A. Ghafoor, and J. L. Alvarado, "Development of hybrid solar distillation system for essential oil extraction," *Renewable Energy*, vol. 113, pp. 22–29, 2017.

[20] W. H. Alawee, H. A. Dhahad, and T. A. Mohamed, "An expermental study on improving the performance of a double slope solar still," in *The 7th International Conference on Sustainable Agriculture for Food, Energy and Industry in Regional and Global Context*, pp. 1–10, Selangor, Malaysia, 2015.

[21] W. H. Alawee, "Improving the productivity of single effect double slope solar still by modification simple," *Journal of Engineering*, vol. 21, no. 8, 60 pages, 2015.

[22] W. H. Alawee, H. A. Dhahad, and K. I. Abass, "Increase the yield of simple solar distillation using the water drip method," *International Journal of Computation and Applied Sciences*, vol. 6, no. 2, pp. 437–486, 2019.

[23] M.'. A. al-Nimr and K. S. Qananba, "A solar hybrid system for power generation and water distillation," *Solar Energy*, vol. 171, pp. 92–105, 2018.

[24] R. Bhardwaj, M. V. ten Kortenaar, and R. F. Mudde, "Influence of condensation surface on solar distillation," *Desalination*, vol. 326, pp. 37–45, 2013.

[25] S. Kiwan, M.'. al-Nimr, and Q. I. Abdel Salam, "Solar chimney power-water distillation plant (SCPWDP)," *Desalination*, vol. 445, pp. 105–114, 2018.

[26] S. W. Sharshir, G. Peng, N. Yang, M. O. A. El-Samadony, and A. E. Kabeel, "A continuous desalination system using humidification - dehumidification and a solar still with an evacuated solar water heater," *Applied Thermal Engineering*, vol. 104, pp. 734–742, 2016.

[27] Z. M. Omara, M. A. Eltawil, and E. A. ElNashar, "A new hybrid desalination system using wicks/solar still and evacuated solar water heater," *Desalination*, vol. 325, pp. 56–64, 2013.

[28] Y. Tian and C. Y. Zhao, "A review of solar collectors and thermal energy storage in solar thermal applications," *Applied Energy*, vol. 104, pp. 538–553, 2013.

[29] G. M. Ayoub, M. Al-Hindi, and L. Malaeb, "A solar still desalination system with enhanced productivity," *Desalination and Water Treatment*, vol. 53, no. 12, pp. 3179–3186, 2015.

[30] S. Abdallah, M. M. Abu-Khader, and O. Badran, "Performance evaluation of solar distillation using vacuum tube coupled with photovoltaic system," *Applied Solar Energy*, vol. 45, p. 176, 2009.

[31] K. Sampathkumar, T. V. Arjunan, P. Pitchandi, and P. Senthilkumar, "Active solar distillation–a detailed review," *Renewable and Sustainable Energy Reviews*, vol. 14, no. 6, pp. 1503–1526, 2010.

[32] A. Allouhi, "Advances on solar thermal cogeneration processes based on thermoelectric devices: a review," *Solar Energy Materials & Solar Cells*, vol. 200, article 109954, 2019.

[33] R. Dev and G. N. Tiwari, "Characteristic equation of a hybrid (PV-T) active solar still," *Desalination*, vol. 254, no. 1-3, pp. 126–137, 2010.

[34] A. E. Kabeel, A. M. Hamed, and S. A. El-Agouz, "Cost analysis of different solar still configurations," *Energy*, vol. 35, pp. 2901–2908, 2010.

[35] Y. Qin, K. Tan, D. Meng, and F. Li, "Theory and procedure for measuring the solar reflectance of urban prototypes," *Energy and Buildings*, vol. 126, pp. 44–50, 2016.

[36] Y. Qin, "Pavement surface maximum temperature increases linearly with solar absorption and reciprocal thermal inertial," *International Journal of Heat and Mass Transfer*, vol. 97, pp. 391–399, 2016.

[37] P. Sharan, T. Neises, J. D. McTigue, and C. Turchi, "Cogeneration using multi-effect distillation and a solar-powered supercritical carbon dioxide Brayton cycle," *Desalination*, vol. 459, pp. 20–33, 2019.

[38] W. H. Alawee, H. A. Dhahad, I. S. Ahmed, and T. A. Mohammad, "Experimental investigation on an elevated basin solar still with integrated internal reflectors and inclined fins," *Journal of Engineering Science and Technology*, vol. 16, no. 1, pp. 762–777, 2021.

[39] W. H. Alawee, H. A. Dhahad, and T. A. Mohammad, "Enhancement of solar still productivity using absorber plate with inclined perforated rectangular fins: experimental study with economic analysis," *Desalination and Water Treatment*, vol. 213, pp. 53–63, 2021.

[40] F. A. Essa, Z. M. Omara, A. S. Abdullah et al., "Wall-suspended trays inside stepped distiller with Al_2O_3/paraffin wax mixture and vapor suction: experimental implementation," *Journal of Energy Storage*, vol. 32, article 102008, 2020.

[41] P. Y. Xiong, A. Almarashi, H. A. Dhahad et al., "Nanomaterial transportation and exergy loss modeling incorporating CVFEM," *Journal of Molecular Liquids*, vol. 330, article 115591, 2021.

[42] B. Mandi, Y. Menni, A. J. Chamkha et al., "Effect of various physical parameters on the productivity of the hybrid distiller - in the time of distillation extension at night," *European Journal of Electrical Engineering*, vol. 21, no. 3, pp. 265–271, 2019.

[43] O. García-Valladares and N. Velázquez, "Numerical simulation of parabolic trough solar collector: improvement using counter flow concentric circular heat exchangers," *International Journal of Heat and Mass Transfer*, vol. 52, pp. 597–609, 2009.

[44] V. Velmurugan, M. Gopalakrishnan, R. Raghu, and K. Srithar, "Single basin solar still with fin for enhancing productivity," *Energy Conversion and Management*, vol. 49, pp. 2602–2608, 2008.

[45] Y. Nurfaidah, I. Wibawa, B. Aprilia, C. Ekaputri, and M. Reza, "Analysis of smart house power savings with on-grid photovoltaic power system," *Journal of Physics Conference Series*, vol. 1367, article 12047, 2019.

[46] P. Sharma, H. Bojja, and P. Yemula, "Techno-economic analysis of off-grid rooftop solar PV system," in *2016 IEEE 6th International Conference on Power Systems (ICPS)*, pp. 1–5, New Delhi, India, 2016.

[47] R. Fares and M. Webber, "The impacts of storing solar energy in the home to reduce reliance on the utility," *Nature Energy*, vol. 2, article 17001, 2017.

[48] A. R. A. Elbar and H. Hassan, "Experimental investigation on the impact of thermal energy storage on the solar still performance coupled with PV module via new integration," *Solar Energy*, vol. 184, pp. 584–593, 2019.

[49] M. Fathy, H. Hassan, and M. Salem Ahmed, "Experimental study on the effect of coupling parabolic trough collector with double slope solar still on its performance," *Solar Energy*, vol. 163, pp. 54–61, 2018.